Petroleum Science 23 (2026) 2950–2962

Contents lists available at ScienceDirect

Petroleum Science

journal homepage: www.keaipublishing.com/en/journals/petroleum-science

Original Paper

Reutilization of regenerated exhaust gas from the centrifugation-filtration coupled purification system: a closed-loop process

Ming Chang, Xin-Lei Li, Yu-Qin Han, Yi-Ping Fan, Chun-Xi Lu *

State Key Laboratory of Heavy Oil Processing, College of Chemical Engineering and Environment, China University of Petroleum (Beijing), Beijing, 102249, China

ARTICLE INFO

Article history:
Received 5 May 2025
Received in revised form
12 August 2025
Accepted 4 January 2026
Available online 6 January 2026

Edited by Min Li

Keywords:
Exhaust gas reutilization
Purification system
Closed-loop process
Pressure drop
Grade efficiency

ABSTRACT

The regenerated exhaust gas was reutilized to configure a centrifugation-filtration coupled purification system (CFCPS), aiming to achieve a closed-loop gas purification process. It can be foreseen that this optimization will bring objective economic savings without sacrificing separation efficiency. A series of typical tests were carried out to analyze the influence of the reutilized exhaust gas on the pressure drop and the separation efficiency. Compared with the purification system without the reutilized exhaust gas, the purifier exhibited optimal performance at $Q = 800$ m^3/h, RV = 25%, and $C_i = 30.24$ g/m^3. Notably, the median size of outlet particles decreased from 1.67 μm to 0.82–1.04 μm and the size range was narrowed when the exhaust gas was recycled. Moreover, the grade efficiency of the dust particles below 3 μm was improved significantly with reutilization. The study indicates that the exhaust gas reutilization is an effective means to solve particle pollution, and further measurements are needed.

1. Introduction

Fluid catalytic cracking (FCC) serves as the main process for heavy oil (high molecular weight and viscosity) conversion in refineries. In the refining process, metal impurities present in the feedstock accumulate on the catalysts due to thermal coking and catalytic coking, which leads to the deactivation of the catalysts and the emission of particulate matter (such as dust particles) (Gambino et al., 2020). When regenerating used catalysts to burn off coke, these metallic contaminants are also transferred into the exhaust gas, ultimately being released into the atmosphere as particulate pollutants (de la Campa et al., 2011). Produced in regenerators operating at 650–750 °C, this gas stream typically contains 12–15 vol% CO_2, 0.5–2 vol% CO, 200–1000 ppm SO_x (dependent on feedstock sulfur content), and <300 ppm NO_x, alongside entrained catalyst fines (50–200 mg/Nm^3, primarily <40 μm particles). Normally, cyclones stand as prevalent solutions for capturing particles in the FCC regenerators. The working principle of the cyclone is centrifugal separation formed by a highly swirling flow (Hoffmann and Stein, 2007). Even though the most advanced inertial gas cleaning systems can capture over 90% of dust particles larger than 5 μm, its performance diminishes notably when confronted with fine–dispersed particles below 2.5 μm (which constitute up to 90% of the total particle amount). Thus, only coarse catalysts can be effectively collected by the cyclone separator. Liu et al. (2012) conducted experimental investigations on a novel "1 + 2" dual-stage cyclone separator, demonstrating. Noh et al. (2018) experimentally integrated multiple auxiliary cyclone units into a tangential inlet separator configuration, which resulted in a significant reduction (over 50%) of fine dust emissions through enhanced particle capture efficiency. Accomplishing the purification requirements is a critical concern for the FCC industry, particularly from a sustainability perspective.

Owing to the low separation efficiency, the mass concentration of dust at the regenerator outlet typically surpasses 150 mg/m^3 and the proportion of the particulate matter below 5 μm is still as high as 75% (Amoatey et al., 2019). As a result, several improved methods have been developed to manage fine dust emissions, such as electro–acoustic ultrasonic nebulization, heterogeneous condensation, electrostatic precipitators, etc. (Zhang et al., 2023). According to the principle of dust removal, it can remove some

* Corresponding author.
E-mail addresses: lcx725@sina.com, lcxing@cup.edu.cn (C.-X. Lu).
Peer review under the responsibility of China University of Petroleum (Beijing).

https://doi.org/10.1016/j.petsci.2026.01.002

particles below 2.5 μm by introducing additional forces. The influence factors on the separation efficiency also increase, such as the residence time, electric field intensity, processing capacity, and so on (Bao et al., 2011). Nevertheless, these technologies require further enhancements, particularly in reducing energy consumption.

After thoroughly evaluating the limitations of the FCC cyclone and recognizing the significant need for improvement, the centrifugation-filtration coupled purification system (CFCPS) is proposed (Lu et al., 2020). The principle of particulate matter removal by this system involves a complex process of centrifugal force and particle filtration, as illustrated in Fig. 1. The cyclone shell was designed on the basis of the PV cyclone, and the built-in granular bed was a coaxial sleeve and the thickness of the interlayer was 50 mm filled with the collector particles. Both the inner and outer walls were made of stainless Johnson screen. Firstly, most large dust particles (>10 μm) are removed from the main downward airflow and strike the outer cyclone wall as a result of centrifugal force. Fine dusts smaller than 10 μm are then retained in the inner granular bed (Chang et al., 2022a). Thus, the cleaned gas was obtained in the outlet duct. The filter media in the built-in granular bed moved downward from the feeder hopper located at the top of the bed to the riser. In the riser, the collector granules as well as the captured fine dust particles were carried into the spouted bed regenerator. The regenerated filter medium re-entered the CFCPS for the next round of dust collection. By combining inertial impaction, interception, gravitation, electrostatic attraction, and Brownian diffusion in the granular bed filter (Pendse et al., 2010), dust particles could be captured in CFCPS efficiently. It is expected to break through the bottleneck of efficient gas–solid separation and eliminate the high-temperature scaling phenomenon of catalytic cracking flue gas turbines.

In a moving bed, a stable or near-stable condition is anticipated when the quantity of dust particles entering the bed matches the amount leaving the bed along with the granules at the filter's base (Colver et al., 2002). The energy consumption and separation performance of the cyclone shell remain almost unchanged under fixed-bed operating conditions. In contrast, the pressure loss of the granular bed increases initially and then reaches a relatively stable or quasi-steady state. From the perspective of the CFCPS, the system pressure drop is mainly influenced by the moving bed filter. To this end, the dust particulates deposited in the bed should be continuously carried out, and the bed filter must be supplemented with sufficient clean particles as the bed particle levels decrease.

To maintain the continuous operation of the CFCPS, the riser-spouted regeneration section is utilized for the collector particles regeneration illustrated in Fig. 1. The filter media, along with the captured dust particles, are transported to the spouted bed via the riser. Because of the variations in material properties, the entrainment velocity of the collector particles is significantly greater than that of the fine dust particles. Consequently, the delivery gas velocity in the riser is set between these two velocities, allowing the mixtures to be efficiently separated in the spouted bed. The regenerated bed filter particles reenter the feeder hopper, while the fine dust particles are discharged into the atmosphere with the exhaust gas (Chang et al., 2024). However, fine dust

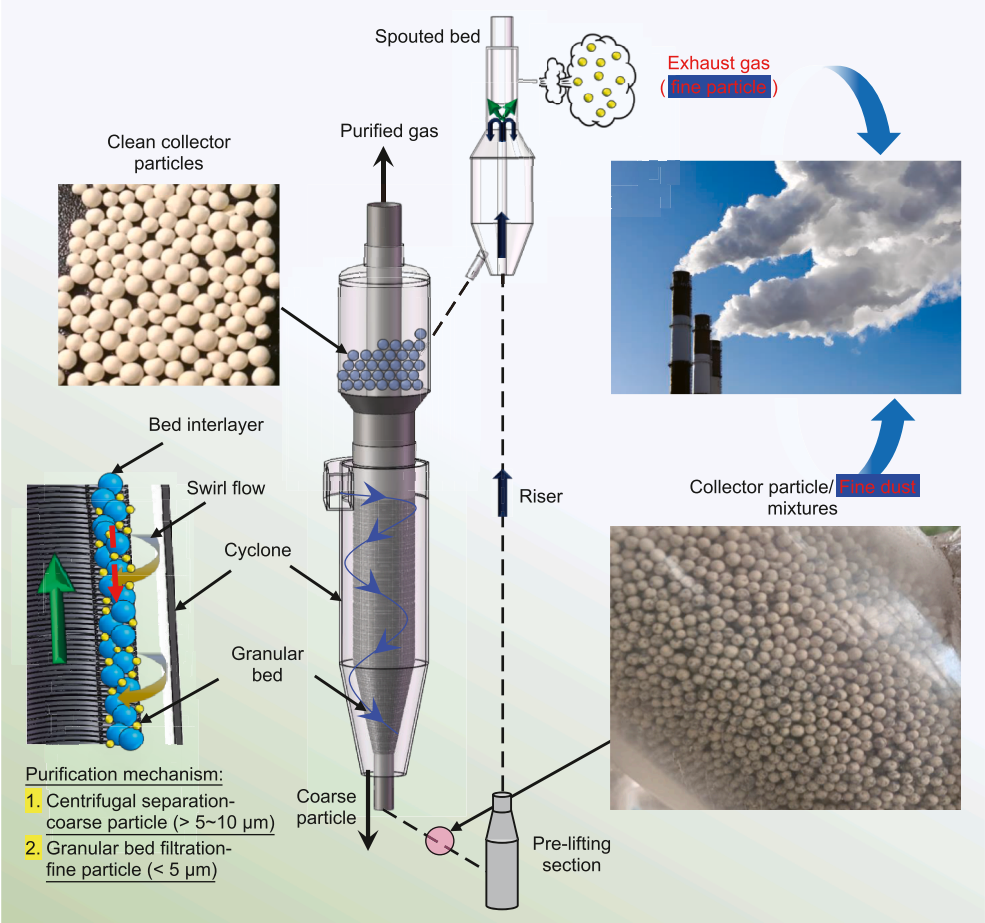

Fig. 1. Schematic of the CFCPS (Chang et al., 2022a).

particles in the regenerated exhaust gas must be collected as much as possible. Overall, the emission refinement issue is still not resolved and a relatively closed-loop gas purification process remains essential.

In previous study (Chang et al., 2022b), the regenerated exhaust gas was purified by a cyclone and a filter bag for post-treatment marked in Fig. 1. However, the separation performance of the small-sized cyclone was limited and the filter bag needed to be replaced frequently. According to previous experiments, filter bags were used worth over 800 USD for exhaust gas purification within 24 h.

Although there are many more efficient technologies for fine dust particles purifying, such as wet scrubbers (Zhao et al., 2024), they are limited in high temperature conditions. The high consumption of experimental supporting materials and environmental issues are obstacles to the implementation of the CFCPS industrial applications. Moreover, the delivery gas volume in the regenerated section opposes approximately 10%–15% of the purified gas volume. If this delivery gas volume were reused, the swirl intensity in the cyclone shell would be enhanced, and the collection efficiency would improve. Because the delivery gas volume in the regenerated section opposes approximately 10%–15% of the purified gas volume. To maintain system efficient separation, about 480 kWh of the electricity used for turbine operation can be saved by exhaust gas reutilization (Tong et al., 1985). Consequently, the probability of reentered fine dust particles being captured would significantly increase in the CFCPS. By reducing system resistance, energy demands for critical equipment like air blowers are gently lowered, allowing operators to reinvest savings into throughput improvements or operational stability. This adjustment also quietly reduces particle attrition, curbing replacement costs and extending equipment longevity in FCC unit. In summary, the reutilization of regenerated exhaust gas is a relatively reasonable approach to achieve a closed-loop gas purification process, considering both device renovation difficulty and energy conservation.

This research work aims to access the reutilization of regenerated exhaust gas from the centrifugation-filtration coupled purification system. Large cold-model experiments were conducted to examine the influence of the reutilized exhaust gas on the purifier, including pressure drop, collection efficiency, outlet particle size, and grade efficiency. FCC industry here was used as the application scenario and the particle medium characteristic adopted in the experiments were same as that in the real industry. Additionally, the optimal operation conditions of the CFCPS were discussed. This study further contributes to the development of environmentally friendly methods for FCC.

2. Experimental

2.1. Experimental platform and methods

A schematic illustration of the primary experimental setup (CFCPS), with exhaust gas reutilization section was shown in Fig. 2. The CFCPS consisted of the centrifugation-filtration purifier, a riser-spouted regenerator, a reutilization pipe, two gas supply devices, and a dust supply device.

The centrifugation-filtration purifier included a cyclone shell and a moving bed filter. The geometric dimensions was presented in Table 1. The cyclone shell was developed by adopting the design principles of the conventional PV cyclone (Alexander, 1949; Mothes and Loffler, 1984; Chen, 2007). In order to observe clearly, the cyclone and the riser-spouted regenerator were constructed of transparent plexiglass produced by Shanghai Yan'an Plexiglass Manufacturing Factory. To optimize the use of swirling flow, the moving bed was positioned at the center of the outer cyclone shell, and both the outer and inner screens were constructed from stainless steel Johnson screens produced by Tangshan Shijia Screen Factory. The path of the swirling flow in the purifier was indicated by a red curve. Most coarse particulates were separated by centrifugal force within the cyclone shell and subsequently fell into the bin. The fine dust particles, carried by the inward swirling flow, were further captured by the moving bed filter. As a result, the gas flow without dust particulate matter was shown in the central outlet.

The gas flow carried dust particles into the purifier system, with dust concentration regulated by a vacuum blower and a screw feeder. The gas flow and dust particle quantities were adjusted to maintain a consistent inlet particle concentration during the experiments. Correspondingly, the dust level in the hopper was also maintained consistently. The mass flow rate of the dust particles was regulated by adjusting the rotational speed (rpm) of the screw feeder. The operation curve of the screw feeder was presented in Fig. 3. To achieve the target inlet dust concentration (7.52, 14.99, 22.50, 30.35, 37.04 g/m^3), the rotational speed of the screw feeder was set to 10, 12, 20, 30 and 37 rpm according to Eq. (1):

$$C_{in} = \frac{k\rho_b v}{Q} \tag{1}$$

where, ρ_b is the particle bulk density, v is the screw rotational speed, Q is the inlet air volume and the correction factor k can be calculated based on the fitting curve shown in Fig. 3..

The experiments were designed to function under suction conditions and negative pressure created by the vacuum blower. The bed particles descended from the feeder hopper and traveled through the moving bed filter. Due to the gravity effect, the mixtures of bed particles and fine dusts flowed into the riser. Accordingly, the circulation velocity of the moving bed filter was established at 5.40 mm/s. The delivery gas was introduced by the air blower and flowed horizontally before entering the spouted bed. The gas volume in the riser was set at 98 m^3/h according to the entrainment velocity difference between the filter media and the dust. In other words, the exhaust gas volume was same to the delivery gas volume. The cleaned collector particles were returned to the feeder hopper through the inclined pipe. The regenerated exhaust gas was transferred to the separator system inlet through the reutilization pipe and a vortex street flowmeter controlled the flow rate. Before the exhaust gas entered the pipe, large dust particles, such as the collector particle debris, were collected by an additional cyclone to prevent the flowmeter blockage. In the experiments, the reflux volume ratio (RV, %) was set at 0%, 25%, 50%, 75%, 100% and the inlet gas volume could be seen as the sum of the gas volume (600, 800, 1000 m^3/h), and the reutilized exhaust gas (98*RV). The corresponding inlet velocity range was also listed in the table. It was worth noting that the flow rate in the reutilization pipe was zero when the reflux volume ratio was set at 0%. The regenerated exhaust gas would be fully discharged. The experimental conditions were presented in Table 2.

The pressure drop in the purifier was determined by measuring the static pressure difference between the inlet and outlet ducts by using a pressure gauge (AZ82062). The data was continuously recorded at 1 Hz. The collection efficiency of the cyclone shell was calculated by Eq. (2):

$$\eta_c = \frac{m_b}{m_{in}} \times 100\% \tag{2}$$

where m_b and m_{in} are the masses of dusts collected by the dust bin and added to the system.

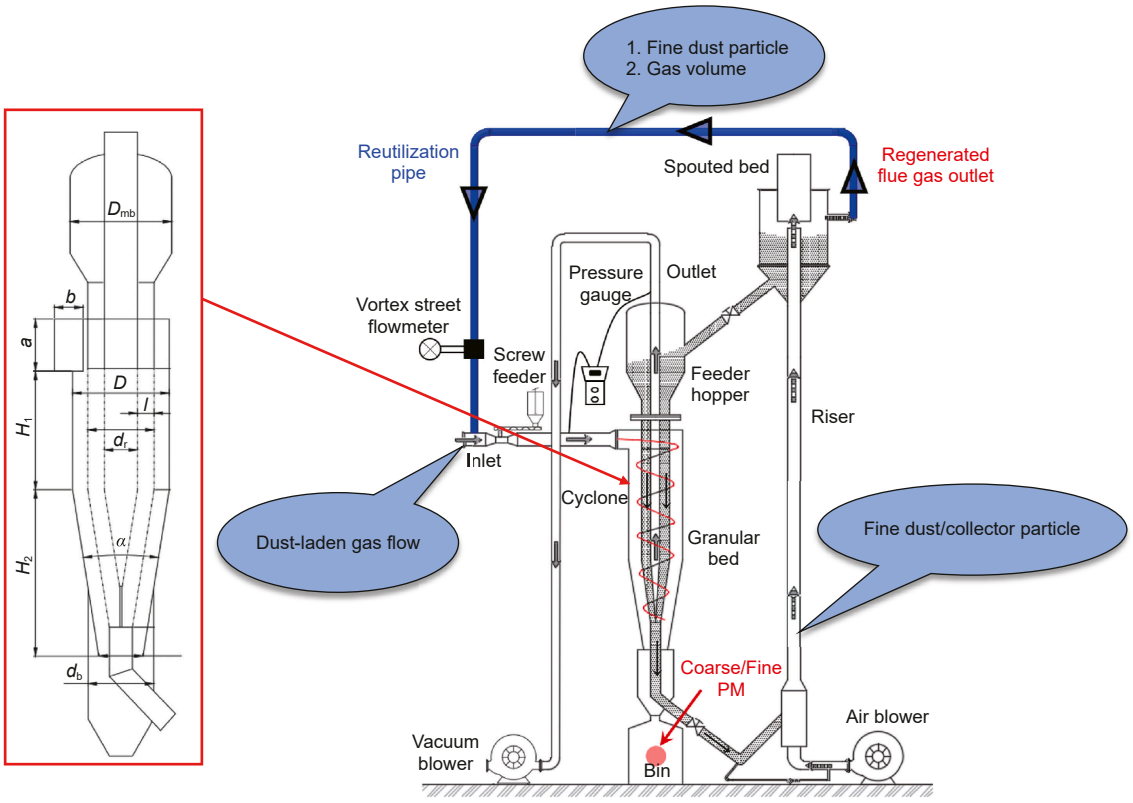

Fig. 2. Schematic of the CFCPS with exhaust gas reutilization section.

Table 1
The geometric dimensions of the centrifugation-filtration coupled purifier.

Parameter	Dimension, mm
Cyclone shell	
Diameter of cyclone shell D	330
Square inlet height a	180
Square inlet width b	84
Height of cylinder H_1	910
Height of cone H_2	609
Diameter of feeder hopper D_{mb}	458
Diameter of dust bin d_b	390
Diameter of outlet pipe d_r	160
Diameter of bottom outlet d_c	182
Angle α	16°
Moving bed filter	
Outer diameter of outer cylinder screen d	243
Inner diameter of dipleg D_d	79

Moreover, the dust particles in the inlet, the dust bin, the outlet, and the reutilization pipe were sampled and then analyzed in a laser analyzer (Model: LS-909, manufactured by OMEC). It should be noted that the sampling method was isokinetic sampling, as explained in previous studies (Chang et al., 2022a). The total collection efficiency was obtained based on the dust concentration difference between the inlet and outlet:

$$\eta = \left(1 - \frac{C_{out}}{C_{in}}\right) \times 100\% \tag{3}$$

where C_{in} and C_{out} are the dust concentrations in the inlet and the outlet.

The efficiency contribution ratio of the centrifugal separation and bed filtration could be obtained:

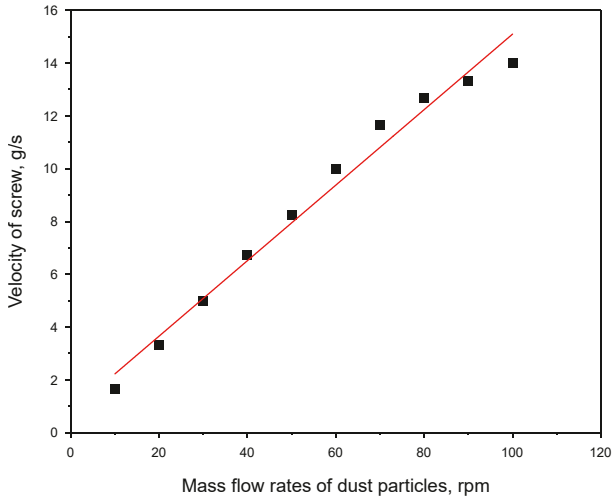

Fig. 3. The operation curve of the screw feeder.

$$\begin{aligned} e_c &= \eta_c \\ e_g &= (\eta - \eta_c)/(1 - \eta_c) \end{aligned} \tag{4}$$

2.2. Materials

Glass beads with average particle sizes of about 1.82 mm were used as the collector particles in the granular bed. The bulk density, the material density and particle density were 2400, 2421 and 1592 kg/m^3, respectively. The dust particles used in this study were FCC catalysts. The size distribution was assessed by the size analyzer. The initial size distribution of the dusts was shown in

Table 2
Experimental conditions investigated within this work.

Number	Inlet gas volume, m^3/h	Inlet gas velocity, m/s	Inlet dust concentration, g/m^3	Exhaust gas volume, m^3/h	Reflux volume ratio RV, %
1	800 + 98*RV	16.53–18.33	7.52	98	0, 25, 50, 75, 100
2	800 + 98*RV	16.53–18.33	14.99	98	0, 25, 50, 75, 100
3	800 + 98*RV	16.53–18.33	22.50	98	0, 25, 50, 75, 100
4	800 + 98*RV	16.53–18.33	30.35	98	0, 25, 50, 75, 100
5	800 + 98*RV	16.53–18.33	37.04	98	0, 25, 50, 75, 100
6	600 + 98*RV	11.02–12.82	14.99	98	0, 25, 50, 75, 100
7	1000 + 98*RV	18.37–20.17	14.99	98	0, 25, 50, 75, 100

Fig. 4. The mass median aerodynamic diameter of the dust particles was found to be 16 μm, adhering to a Gaussian distribution. The particle size distribution and the median particle diameter were measured by a laser particle size analyzer (LS-909, manufactured by Zhuhai OMEC instruments Co., Ltd).

3. Results and discussion

3.1. The performance of the riser-spouted bed regenerator

To assess the impact of the exhaust gas reutilization on the purifier, the regeneration performance of the riser-spouted bed regenerator should be investigated first. The spouted regeneration achieved the fine dust and coarse particles separation based on the particle properties variation. The delivery gas volume in the riser was set based on the calculated airflow entrainment velocity and the volume was almost unchanged. The dust concentration at the inlet of the purifier affected the regeneration efficiency, correspondingly. In other words, the dust concentration entering the regenerator mainly depended on the dust particulates captured by the moving bed filter. Based on earlier studies (Chang et al., 2022a, 2024), the filtration efficiency of the moving bed was enhanced by increasing dust concentration. Hence, the dust/collector particles mixtures were sampled before and after the regeneration and then these samples were screened by a standard sieve. By analyzing the particle size distribution, the regeneration efficiency could be calculated by Eq. (5):

$$\eta_r = \frac{f_b - f_a}{f_b} \times 100\% \quad (5)$$

where f_b and f_a are the mass ratios of the dust particulates and the collector particles sampled at the beginning/end of the regeneration process.

As illustrated in Fig. 5, the mass ratio increased with the inlet dust concentration correspondingly when RV = 0%, leading to an improvement in regeneration efficiency. The regeneration efficiency was maintained at about 81% with low inlet dust concentration. Due to the separation performance induced by the centrifugal mechanism was limited, an increase in inlet dust concentration led to a higher entrainment of fine dust particles into the moving bed filter. The mixtures, including the fixed quantity collector particles (the circulation velocity in the moving bed was fixed) and large amounts of dusts were transported into the regenerator. The entrainment velocity in the riser-spouted bed regenerator was set in reference to the dust-entrained velocity and the difference was significant. Therefore, the mass ratio after the regeneration process increased slightly. The performance of the purifier and the regenerator exhibited a limited effect on the regenerated exhaust gas. The relatively stable exhaust gas was the foundation for achieving reutilization in CFCPS.

In the purifier, coarse dusts (≥10 μm) were separated in the cyclone and fine dust particles (<10 μm) were filtrated in the moving bed. The amount of fine dusts in the purifier inlet increased when the exhaust gas was reutilized. In this condition, the performance of the purifier was influenced consequently. By sampling the dust particles in the reutilization pipe, the particle size distribution analysis results were illustrated in Fig. 6(a). As for the regenerated exhaust gas was purified preliminarily, the median particle size was between 0.82 and 1.04 μm. According to the size analysis, the inlet dust distribution, including the dust

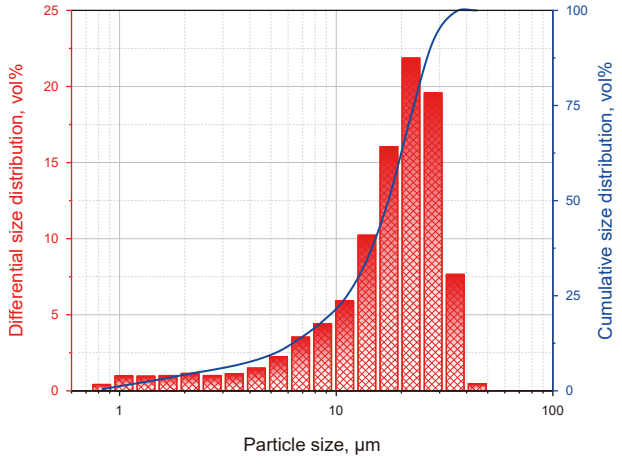

Fig. 4. Size distribution of FCC catalysts.

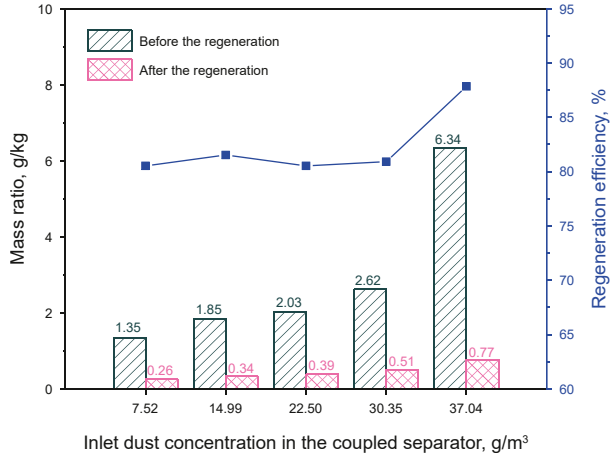

Fig. 5. The dust mass ratio before and after the regeneration and the regeneration efficiency at various inlet dust concentrations (RV = 0%).

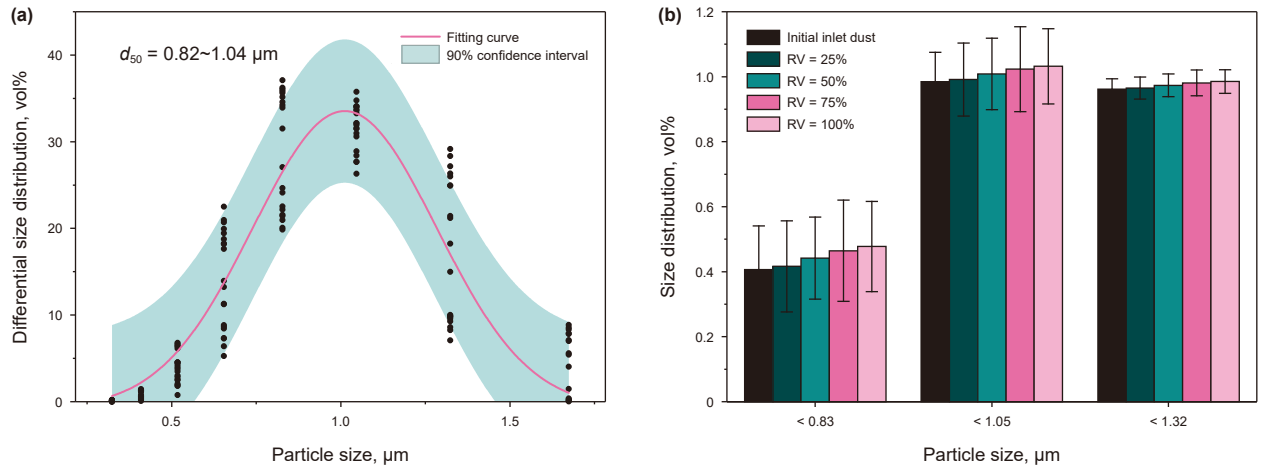

Fig. 6. The size distribution in the exhaust gas with different reflux volume ratio. **(a)** Whole particle size distribution. **(b)** Size distribution below 1.32 μm.

particles from the screw feeder and the reutilization pipe, could be computed and the results were also summarized in Fig. 6(b). The inlet size distribution was influenced by the exhaust gas mainly on the particles below 1.32 μm. Although the increment was not substantial, the fine dust particles were an important component of the dust cake formation. By reutilizing the regenerated exhaust gas, especially the airflow volume and fine dust particles, the centrifugal separation and the bed filtration would be both improved accordingly. Thus, the downstream operation unit equipment lifespan is extended by avoiding particle wear and coking in FCC industry. Moreover, a closed-loop gas purification process was likely to be achieved. These cost savings, combined with reduced regulatory non-compliance risks, position CFCPS as both an environmentally and financially sustainable solution.

Concerning the inlet dust particles, the dust size distributions at the beginning/end of the regeneration process were compared in Table 3. It seems that the dust size distribution before and after regeneration tended to be consistent, and the median size increased about 0.6 μm after regeneration. Two reasons could be attributed to the difference. Firstly, part of fine dust particles was carried out with the exhaust gas. Conversely, high gas velocity in the riser caused significant attrition of the bed particles, which interfered with the size analysis due to the debris. For example, particles larger than 10 μm were found in the mixtures after the regeneration. In general, the amount of fine dust particles and particle size returned to the purifier was greatly relevant to the regenerated exhaust gas reflux volume ratio. Further experimental investigation is imperative to validate theoretical models and elucidate underlying mechanisms.

Based on above results, the potential of the exhaust gas reutilization was confirmed preliminary on the performance improvement of the CFCPS. Firstly, a higher total airflow volume enhances the centrifugal separation and swirl intensity in the cyclone shell. For the moving bed filter, the changes in bed porosity and the dust cake resulting from the deposition of fine particles were advantageous for particle filtration. The chain effect in the recycling loop process, involving the purifier, regenerator, and regenerated exhaust gas, is discussed with a focus on separation performance.

3.2. The variation in the pressure drop

Pressure drop serves as a critical parameter for assessing device applicability, directly governing operational flexibility and economic feasibility. Fig. 7 illustrated the pressure drop sequences over time for various inlet dust concentrations and reflux volume ratios. Clearly, the pressure drop of the purifier was comprehensively determined by multiple factors and which factor played the dominant role depending on the specific operation conditions. As shown in the chart, significant differences could be observed. When the inlet dust concentration was low (C_i = 7.52 g/m^3), the pressure drop rose as the dust–laden operation progressed. Compared to RV = 0%, the overall value increased with the reflux volume ratio. It appeared that the influence of the exhaust gas volume was indistinct as the reflux volume ratio increased. The dust particles below 5 μm from the exhaust gas became the dominant factor. As the fine dust particles escaped from the swirling flow, they were intercepted in the moving bed by several

Table 3
Particle size distribution of the dusts sampled before and after the regeneration.

Inlet dust concentration, g/m^3	7.52		14.99		22.50		30.35		37.04	
size, μm	Before	After	Before	After	Before	After	Before	After	Before	After
0~1	0.50	0.45	0.79	1.12	0.73	1.17	0.45	0.95	0.25	3.69
1~2	5.70	1.81	5.90	3.05	5.80	2.06	4.66	3.61	6.67	6.97
2~4	6.48	9.85	10.08	6.12	9.04	4.59	6.00	6.01	10.88	36.35
4~6	27.78	32.99	31.22	16.81	31.42	11.77	24.45	13.44	31.92	44.54
6~8	48.91	47.38	43.14	38.14	46.52	32.40	48.28	36.79	44.63	8.46
8~10	22.28	19.36	18.59	21.26	19.89	19.53	24.03	21.35	18.72	0.90
>10	10.63	7.52	8.88	31.48	6.49	39.54	16.15	35.68	5.65	0
d_{50}	6.1	6.2	6.2	7.1	6.0	7.3	6.4	7.2	6.1	6.4

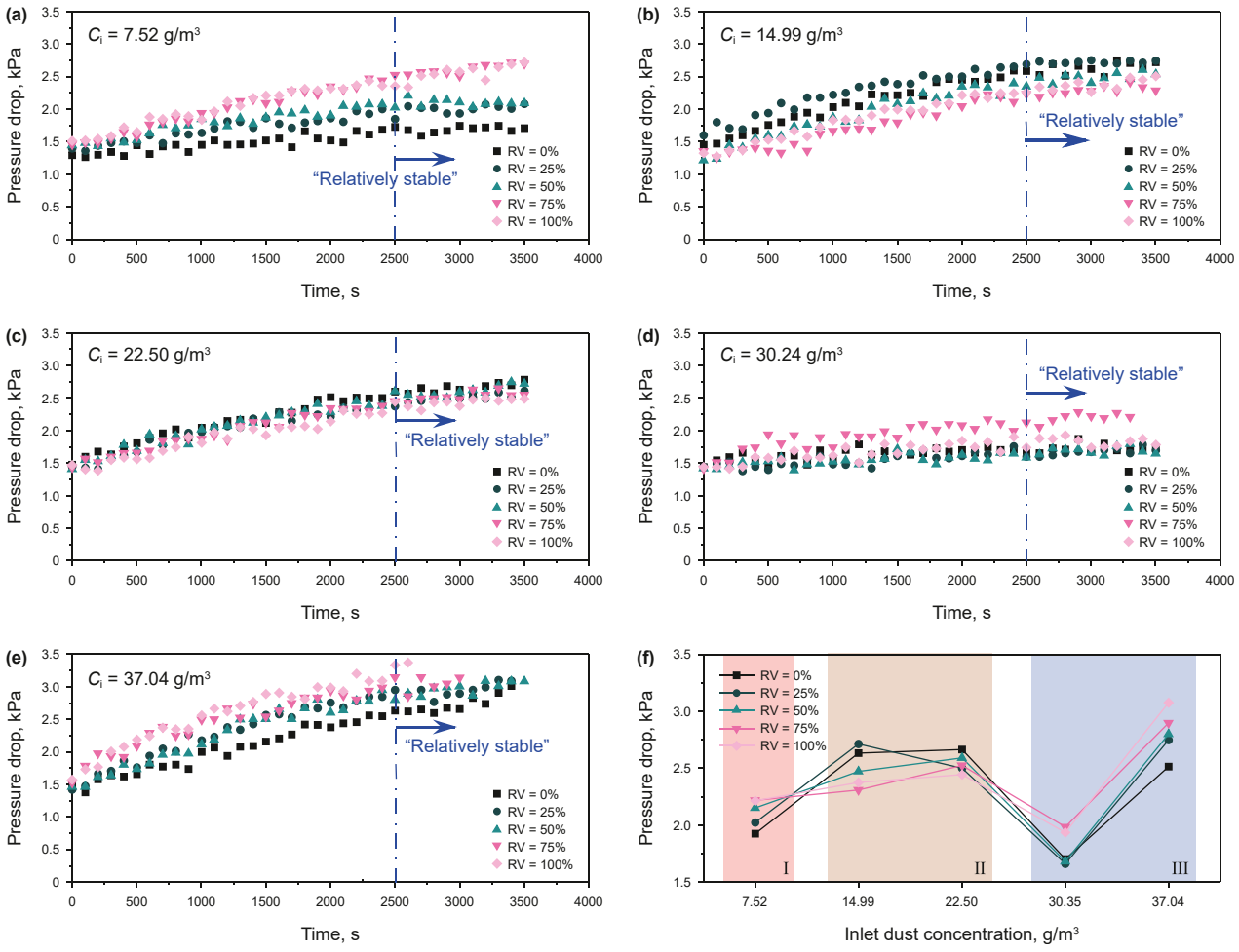

Fig. 7. The pressure drop sequences of the purifier with different inlet dust concentrations and reflux volume ratios. **(a)** $C_i = 7.52$ g/m^3, **(b)** $C_i = 14.99$ g/m^3, **(c)** $C_i = 22.50$ g/m^3, **(d)** $C_i = 30.24$ g/m^3, **(e)** $C_i = 37.04$ g/m^3. **(f)** Average pressure drop.

filtration mechanisms. While the pressure drop tendency with RV = 75%/100% was almost identical, the dust cake that formed on the bed screen could be alleviated by the self-cleaning phenomenon, as demonstrated in previous study (Chang et al., 2022a).

However, different growth gradients could be seen at $C_i = 14.99$ g/m^3 in Fig. 7(b). The pressure drop in the separator rose by approximately 0.14 kPa before reaching a reflux volume ratio of 25%. And then a clear decrement could be observed from RV = 25%–100%. It was clear that the impact of fine dusts from the reutilized exhaust gas became weak with the inlet dust concentration increasing. The variation tendency was maintained in Fig. 7(c). The inlet dust concentration was the dominant factor compared to the pressure drop with $C_i = 7.52$ g/m^3. Furthermore, the gas volume from reutilized exhaust gas could be seen as the secondary dominant factor. In this case, the pressure loss in the moving bed increased due to the limited improvement of the centrifugal separation. The pressure loss variations with high inlet dust concentrations in Fig. 7(d) and (e) exhibited other characteristics. A positive correlation was observed between the pressure drop and the exhaust gas reflux volume ratio. According to the large interaction force between dust particles, the agglomeration phenomenon existed in the separation process. Under the combined effect of the initial inlet dust-laden gas and the exhaust gas, the swirling fluid friction loss (Alexander, 1949; Mothes and Loffler, 1984) in the cyclone shell and the moving bed filter pressure drop both increased.

For better analysis of the exhaust gas reutilization, the average pressure drop at different operation conditions was depicted in Fig. 7(f). Once the dust in the bed reached a dynamic equilibrium between deposition and removal, the pressure drop remained relatively constant after 2500 s according to Fig. 7(a)–(e), and this phenomenon was considered as the relatively stable state. Thus, the typical pressure drop compared in Fig. 7 was obtained by the average value of the relative stable data among 2500–3500 s.

In terms of the dominant factors discussed above, three regions were distinguished and marked in Fig. 7(f). It was notable that the pressure drop achieved the lowest at $C_i = 30.24$ g/m^3. In the first region, the increase in fine dusts content forced an increase in pressure losses. With the inlet dust concentration increasing, the influence of the fine particle component and the exhaust gas volume both took effect in the second region. In the last resort, the influence of fine dust in the exhaust gas was mitigated by a high initial inlet dust concentration. The exhaust gas volume became the relative dominant factor in the third region regarding the reflux volume ratio. The above results altogether indicated that the purifier features affected by the reutilization of the exhaust gas should be applied considering the operation conditions.

As shown in Fig. 8(a)–(e), the pressure drop of the purifier with different inlet gas volumes was compared. It was observed that as the inlet gas volume increased, both the pressure drop and data fluctuations rose significantly. Due to the consistent inlet dust concentration, the swirling fluid friction loss increased

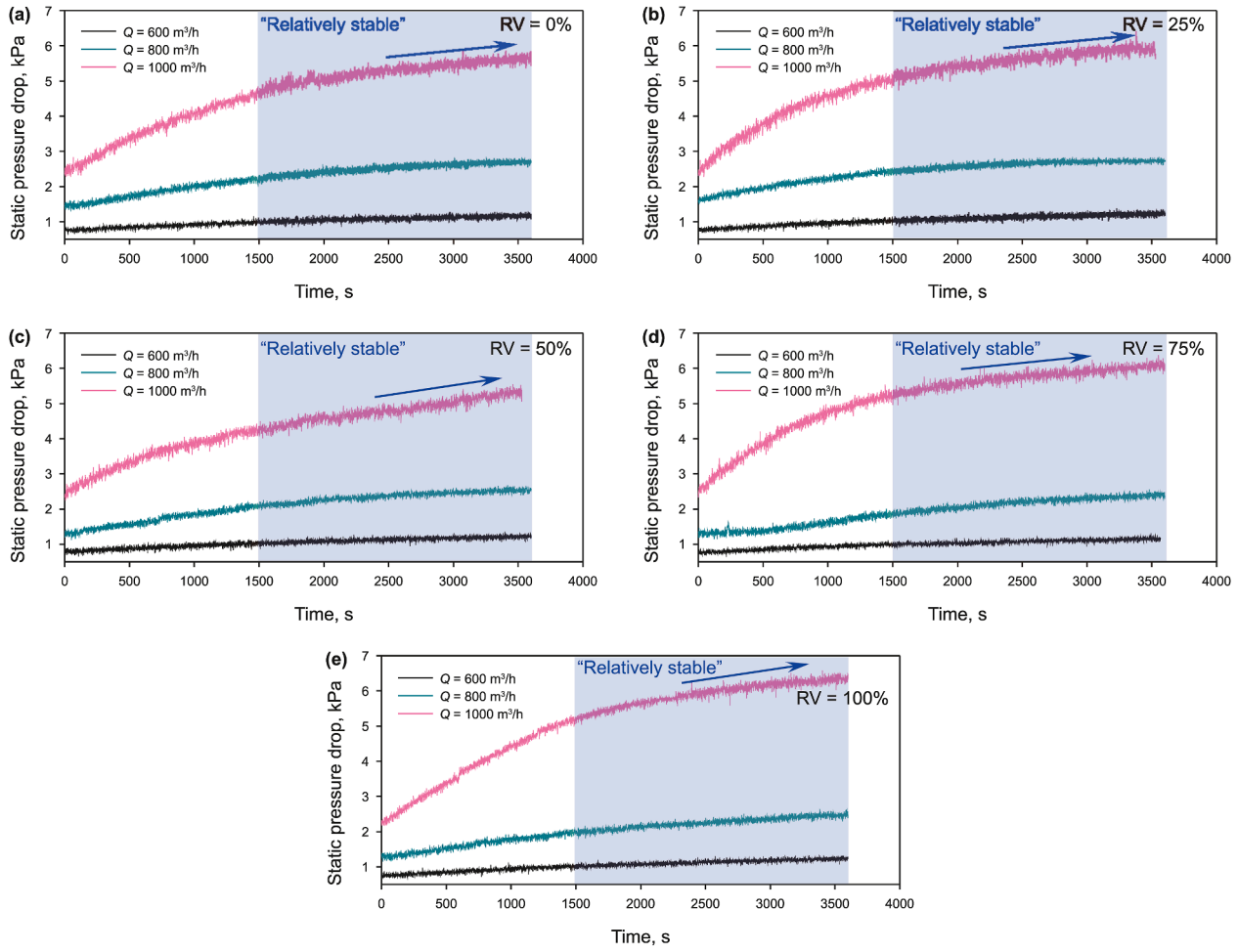

Fig. 8. The pressure drop sequence of the purifier with different inlet gas volume and reflux volume ratios. **(a)** RV = 0%, **(b)** RV = 25%, **(c)** RV = 50%, **(d)** RV = 75%, **(e)** RV = 100%.

exponentially with the swirling velocity in the cyclone shell. Moreover, the outer screen of the moving bed filter strengthened this effect. Besides, the swirl intensity in the cyclone shell and the cross-flow in the bed were both enhanced as the swirling flow velocity increased and the formation of dust cake in/on the moving bed was suppressed. It was important to note that the residence time in the swirl space also decreased. The possibility of fine dust particles entering the granular bed grew. After that, it was shown that large pressure drop growth occurred at a high reflux volume ratio. Consequently, modulating the reflux rate within optimized thresholds prevents excessive equipment pressure drop escalation, while strategically tolerating marginal efficiency losses proves paramount for maintaining systemic operational stability.

3.3. Collection efficiency in the purifier

In addition to considering pressure drop, separation efficiency is another crucial parameter. Fig. 9 showed the collection efficiency at various inlet dust concentrations and reflux volume ratios. The total collection efficiency exceeded 992‰. The most important thing was that the efficiency was improved dramatically with the introduction of the regenerated exhaust gas. Interestingly, the purifier under $C_i = 14.99$ g/m^3, RV = 25% achieved the highest collection efficiency. In other words, the optimum operating condition was discovered without considering the pressure drop temporarily. It was meaningful to study the reason that

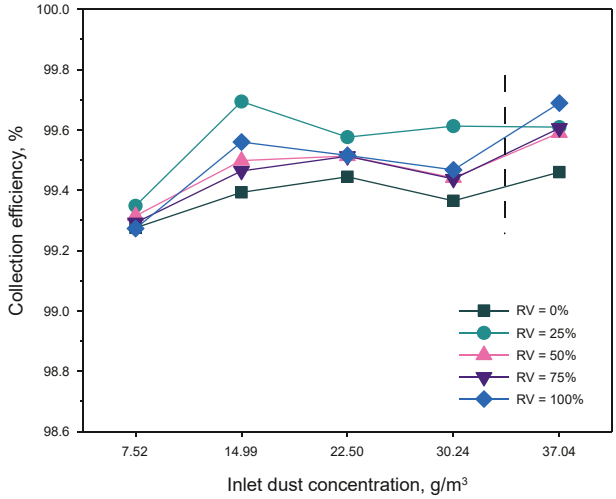

Fig. 9. The collection efficiency of the purifier with different inlet dust concentrations and reflux volume ratios.

affected the collection performance and further improve it in terms of the separator pressure loss. When the inlet dust concentration was 7.52 g/m^3, the collection efficiency increased slightly compared to RV = 0%. As the inlet dust concentration

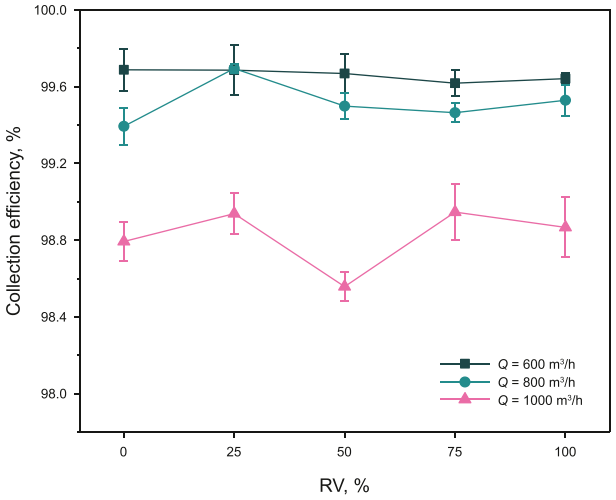

Fig. 10. The collection efficiency of the purifier with different inlet gas volume and reflux volume ratios.

increased, the differences between various reflux volume ratios became more pronounced. Comparison of the reutilized exhaust gas influence below $C_i = 30.24$ g/m^3 showed similar efficiency results: the fine dust concentration and gas volume with RV = 25% ensured that the coupled purifier exhibited the best separation characteristics. For the purifier, the improvement of centrifugal separation efficiency meant that the amount of dust particles entering the moving bed filter was correspondingly reduced, and then the bed filtration was affected. More fine dust particles from the exhaust gas entered the bed filter directly through the cyclone shell, and the decrease in bed porosity compensated for the negative effect of "low volume efficiency". On the other hand, high exhaust gas reutilization value increased the swirl intensity and the residence time of dust in the cyclone shell was shortened. The decrease in residence time reduced the possibility of the dust particles captured by the centrifugal mechanism. As mentioned above, the exhaust gas volume became the relative dominant factor when $C_i = 37.04$ g/m^3. Considering the particle agglomeration characteristic, high separation efficiency was achieved in the cyclone shell especially when the regenerated exhaust gas was all reutilized.

The experimental results about the effect of the inlet gas volume and reflux volume ratio on the collection efficiency were presented in Fig. 10. Overall, the collection efficiency decreased with the inlet gas volume increasing. Although coarse dust particles separation was enhanced in the cyclone shell, the total collection efficiency was compromised by increased fine dust particles content from the exhaust gas. It was clear that the impact of the exhaust gas reflux volume ratio on collection efficiency differed with varying inlet gas volumes. At low inlet gas volume

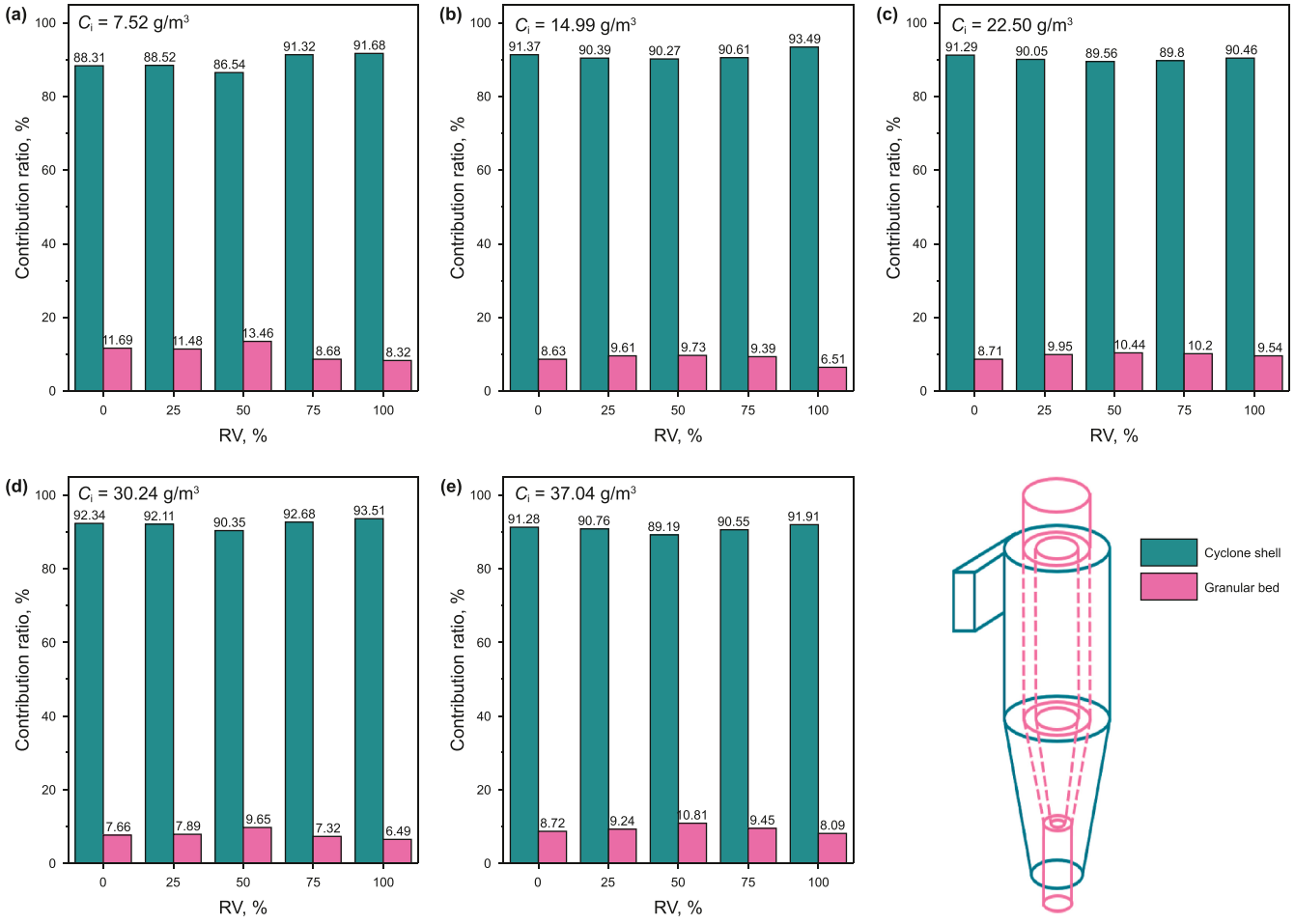

Fig. 11. The contribution ratio of the cyclone and the moving bed at varying inlet dust concentrations and reflux volume ratios. **(a)** $C_i = 7.52$ g/m^3, **(b)** $C_i = 14.99$ g/m^3, **(c)** $C_i = 22.50$ g/m^3, **(d)** $C_i = 30.24$ g/m^3, **(e)** $C_i = 37.04$ g/m^3.

(Q = 600 m^3/h), the collection efficiency remained above 995‰ due to the high proportion of the reutilized exhaust gas in the total inlet gas volume. Compared to other operation conditions, the dust cake filtration was enhanced by the dust particle deposition and the weaker swirl flow cleaning effect. While the collection efficiency at Q = 1000 m^3/h was below 99%. Additionally, an obvious minimum value was shown at RV = 50%. The collection efficiency enhanced by the gas volume from the regenerated exhaust gas could not cope with the entrained fine dust particles.

To figure out the effect of the reutilized exhaust gas on the centrifugal separation and bed filtration respectively, the efficiency contributions ratio under different inlet dust concentrations and reflux volume ratios were illustrated in Fig. 11(a)–(e). Clearly, the cyclone shell captured approximately 90% of dusts, which was crucial for gas purification. Additionally, the contribution ratio increased with rising inlet dust concentration. This enhanced contribution from the cyclone shell alleviated the load on the subsequent granular bed, helping to maintain high bed porosity. The operating cycle of the coupled equipment was extended because the filtration pressure loss was also reduced. The median particle size in the dust bin was around 22.15 μm (larger than the initial inlet dust particle size), with a particle size range of 4.28–44.82 μm. The dust particles above 10 μm accounted for more than 92%, which was related to the characteristic of the centrifugal separation mechanism in the cyclone.

More importantly, the minimum value of the cyclone contribution ratio frequently appeared at RV = 50% under different inlet dust concentrations. Relatively speaking, the opposite trend occurred in granular bed filtration. It had been pointed out above that the fine dust concentration and gas volume from the reutilized exhaust gas at RV = 50% were the intermediate value. Thus, it could be concluded that the centrifugal force was enhanced by high inlet mixed gas flow when RV<50%. At the same time, fine dust particles were collected efficiently. However, the centrifugal separation efficiency was weakened as the limited increase in reutilized exhaust gas volume at RV = 50%. Considering the agglomeration, the separation process in the cyclone shell recovered as RV > 50% and exceeded the efficiency at RV < 50%. Moreover, the increasing content of fine dust particles below 2 μm helped the dust cake formation in the granular bed. While the cake would be destroyed by high tangential gas flow from the cyclone shell. By adjusting the exhaust gas reflux volume ratio, the performance advantages of the purifier became more apparent based on the corresponding operating conditions. This is also the reason why it is necessary to conduct pilot-scale experiments to address the equipment operating characteristics, thus bridging the critical knowledge gap between laboratory findings and industrial process scalability.

As discussed above, the efficiency contribution of the centrifugal separation was improved by increasing the inlet gas volume. The calculated results were illustrated in Fig. 12(a)–(e). Because of this phenomenon, the dust particles that escaped from the centrifugal separation was weakened. Changes in bed porosity and dust cake in the granular bed were slight, the filtration efficiency

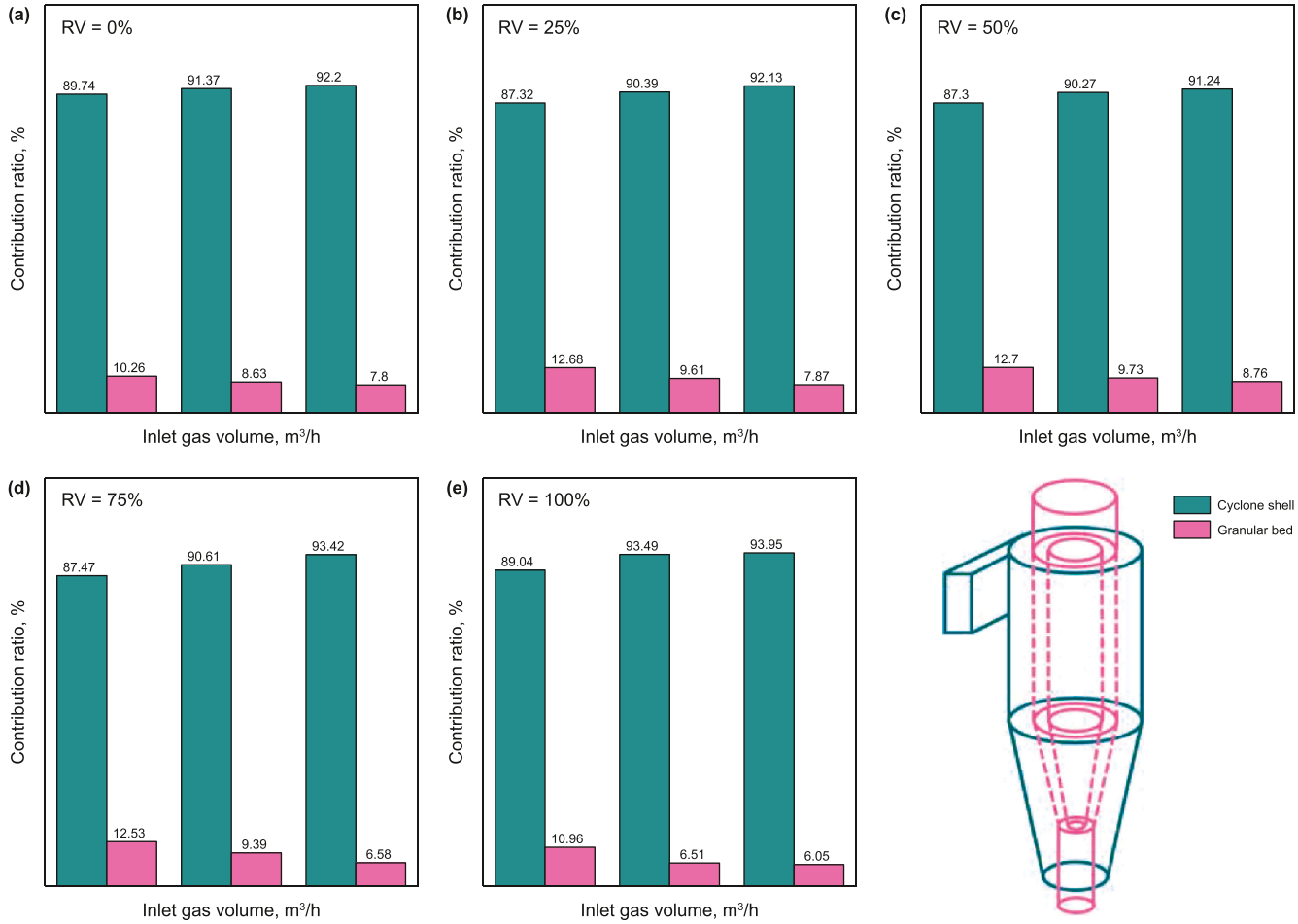

Fig. 12. The contribution ratio of the cyclone and the moving bed with different inlet gas volume and reflux volume ratios. **(a)** RV = 0%, **(b)** RV = 25%, **(c)** RV = 50%, **(d)** RV = 75%, **(e)** RV = 100%.

decreased with increasing inlet gas volume. From the perspective of pressure loss, the variation of the moving bed filtration pressure induced a limited impact on the overall pressure loss. It appears that the gas volume from the exhaust consistently had a positive effect on dust particle collection. While the fine dust particles were separated more efficiently at a high reflux volume ratio.

In addition, the outlet size distribution with different inlet concentrations and reflux volume ratios was also presented in Fig. 13. The median size remained almost unchanged when the reflux volume ratio was greater than 0%. Compared to RV = 0%, the median size decreased from 1.67 μm to 0.82–1.04 μm with a narrower size range. Thanks to the dust cake enhancement and the swirling flow strengthening, the dust particles could be separated efficiently. The size analysis indicated that the reutilization of the exhaust gas was beneficial to the purification of dust particles. The designed reutilization pipe was expected to the optimization of

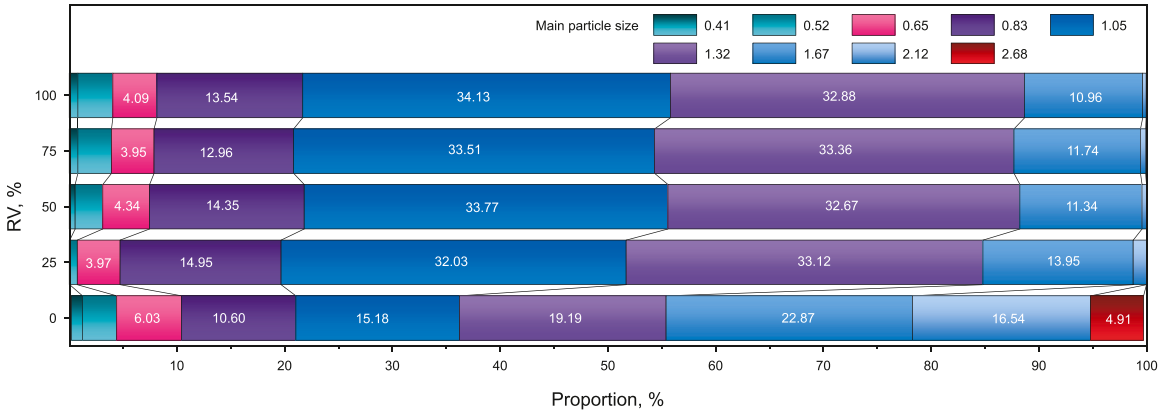

Fig. 13. The outlet size distribution with different inlet dust concentrations and reflux volume ratios.

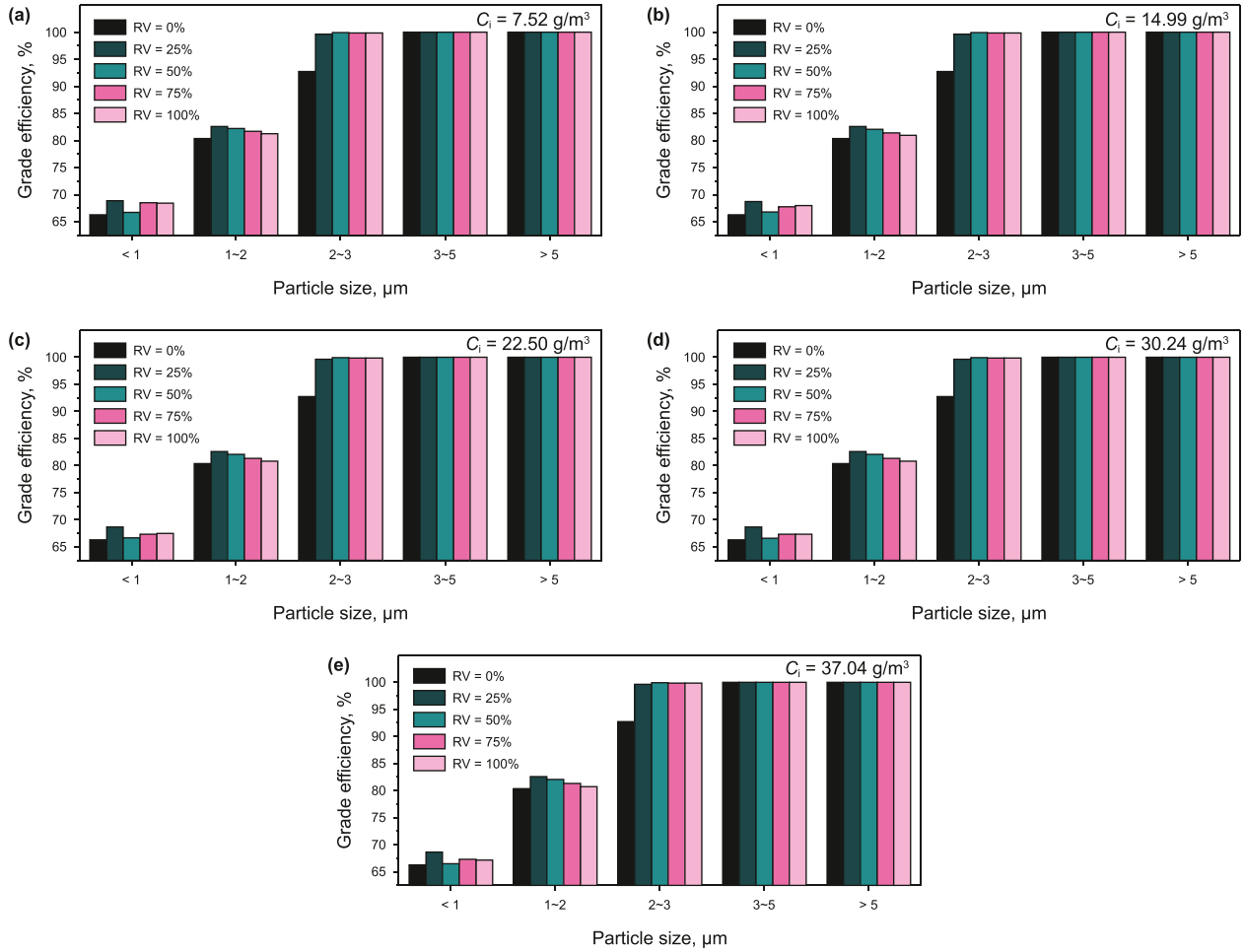

Fig. 14. The grade efficiency with different inlet dust concentrations and reflux volume ratios **(a)** C_i = 7.52 g/m^3, **(b)** C_i = 14.99 g/m^3, **(c)** C_i = 22.50 g/m^3, **(d)** C_i = 30.24 g/m^3, **(e)** C_i = 37.04 g/m^3.

exhaust gas purification and recovery technology for a closed-loop gas purification process. For technology providers, the CFCPS opened a collaborative path to innovate and deliver solutions that balance efficiency with sustainability. Environmentally, the reduction in energy use and particulate emissions aligns.

3.4. The grade efficiency in the purifier

The obtained outlet dust was further utilized for analyzing the purifier performance. Based on the size distribution, the grade efficiency could be calculated by Eq. (5):

$$\eta_i = 1 - (1-\eta)\frac{f_o(\delta_x)}{f_i(\delta_x)} \tag{5}$$

where, $f_o(\delta_x)$ and $f_i(\delta_x)$ represented the proportion of the dust particle size δ_x in the outlet and inlet.

As shown in Fig. 14(a)–(e), by comparing the typical size range concerned in the industry, it could be found that the grade efficiency of the dust particles below 3 μm was improved significantly, up to 7%, by reutilizing the regenerated exhaust gas. Numerous references have confirmed that high efficiency in the cyclone separator was limited below 5 μm, the centrifugal separation was compensated by the introduction of the moving bed filter (Chang et al., 2022a; Chang et al., 2024b). The lower limit was extended to 2–3 μm. Besides, the impact of the inlet dust concentrations increased slightly because of the fine particle characteristics.

For the dusts below 1 μm, the best separation performance occurred at RV = 25% and a relatively worse condition was shown at RV = 50% despite no exhaust gas recycling. Concerning the particle size between 1–2 μm, the grade efficiency achieved about 81%. The tendency was similar to that of finer particles. As mentioned in Chapter 3.3, the collection efficiency of the purifier was affected by the combined effect of the fine dust particles and volume from the exhaust gas. As the reflux volume ratio increased, the centrifugal force intensified, causing dust particles that had been left in the bed or adhered to the screen wall to be dislodged. When RV = 50%, the content of fine dust particles increased compared to RV = 25%. However, the self-cleaning phenomenon induced by the swirl flow was not effective. In other words, the fine dust particles escaped the centrifugal separation and bed filtration. Considering the pressure drop variation, the optimum operation condition of the purifier should be RV = 25% and C_i = 30.24 g/m^3. The effect of the exhaust gas reutilization on the CFCPS would provide some guidance and advice on the improvement of the closed-loop gas purification process.

Fig. 15 presented the grade efficiency of the purifier with different inlet gas volume and reflux volume ratios. Comparing the efficiency columns, the grade efficiency with Q = 600 and 800 m^3/h was higher than that with Q = 1000 m^3/h, especially for fine dust particles below 2 μm. According to classical particle classification theory, grade efficiency typically decreases with smaller particle sizes (Klimpel, 1982; Hoffmann and Stein, 2007). As a result, small dust particles experienced less centrifugal force and were more likely to escape from the cyclone (Roldán–Villasana et al., 1993; Minkov et al., 2014). High cross-flow velocity was maintained in the moving bed filter and the deposited dusts between the collector particles was carried out. This would result in a relatively low separation efficiency of fine particles. It was noteworthy that the grade removal efficiency for 2–3 μm dust particles increased with the RV. This was consistent with the results mentioned in Chapter 3.3. By controlling operating conditions such as inlet gas volume and exhaust gas reflux volume ratio, the performance of the CFCPS can be adjusted to meet various product classification objectives, which is also the focus of ongoing research.

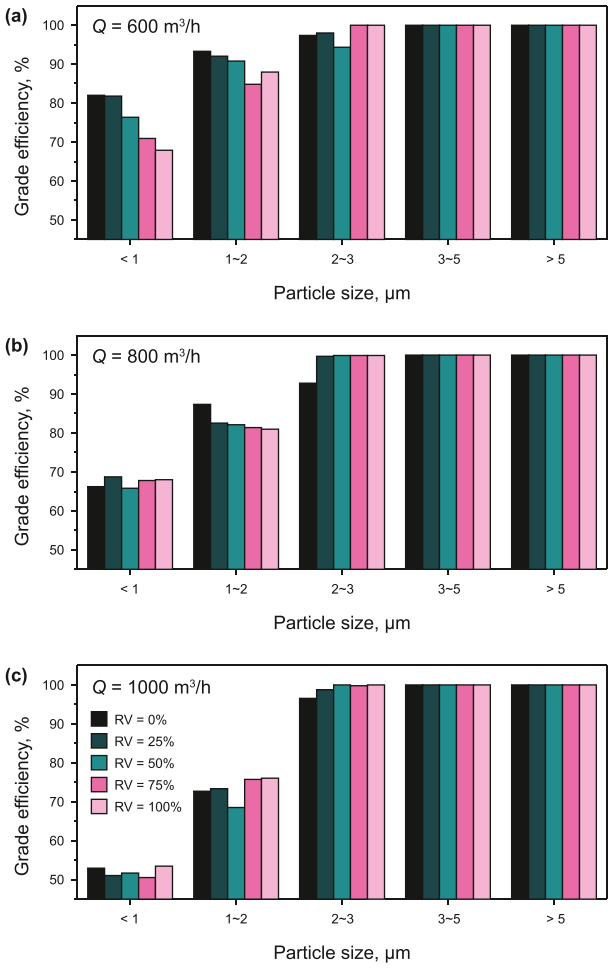

Fig. 15. The grade efficiency of the purifier with different inlet gas volume and reflux volume ratios. **(a)** Q = 600 m^3/h, **(b)** Q = 800 m^3/h, **(c)** Q = 1000 m^3/h.

4. Conclusion

In this study, regenerated exhaust gas was reutilized in a novel centrifugation-filtration coupled purification system (CFCPS) to establish a closed-loop gas purification process. The purifier demonstrated optimal performance at a flow rate (Q) of 800 m^3/h, a reflux volume ratio (RV) of 25%, and an inlet dust concentration (C_i) of 30.24 g/m^3. Further analysis revealed that fine dust particles and exhaust gas volume were critical factors affecting the pressure drop, with their impact varying based on the inlet dust concentration. Compared to the baseline condition (RV = 0%), the median particle size at the outlet decreased from 1.67 μm to a range of 0.82–1.04 μm, accompanied by a narrower particle size distribution. Additionally, the grade efficiency for dust particles smaller than 3 μm was significantly enhanced through reutilization. From the obtained analysis, it was evident that the centrifugal separation and granular bed filtration were both strengthened by the fine particles and gas volume from the exhaust gas. These findings offer valuable insights for optimizing closed-loop gas purification processes in analogous systems. Compelling all altogether, this waste reutilization taught us a way to save the environment or industry pollution problem by exploring the pollution source.

CRediT authorship contribution statement

Ming Chang: Writing – review & editing, Writing – original draft, Visualization, Validation, Project administration,

Methodology, Investigation, Funding acquisition, Conceptualization. **Xin-Lei Li:** Formal analysis, Data curation. **Yu-Qin Han:** Formal analysis, Data curation. **Yi-Ping Fan:** Validation, Supervision. **Chun-Xi Lu:** Validation, Supervision.

Declaration of competing interest

The authors declare that they have no known competing financial interests or personal relationships that could have appeared to influence the work reported in this paper.

Acknowledgement

The financial support received from supported by National Natural Science Foundation of China (Grant number: 22408396); Science Foundation of China University of Petroleum, Beijing (Grant number: 2462023XKBH010).

References

Alexander, R., 1949. Fundamentals of cyclone design and operation. Proc. Australas. Inst. Min. Metall. 152–153, 203–228.

Amoatey, P., Omidvarborna, H., Baawain, M.S., Al-Mamun, A., 2019. Emissions and exposure assessments of SO_x, NO_x, dust particles 10/2.5 and trace metals from oil industries: A review study (2000–2018). Process Saf. Environ. Prot. 123, 215–228. https://doi.org/10.1016/j.psep.2019.01.014.

Bao, J., Yang, L., Sun, W., Geng, J., Yan, J., Shen, X., 2011. Removal of fine particles by heterogeneous condensation in the double-alkali desulfurization process. Chem. Eng. Process. Process Intensif. 50, 828–835. https://doi.org/10.1016/j.cep.2011.05.008.

Chang, M., Fan, Y., Fu, J., et al., 2022a. A model for predicting the separation performance of a coupling cyclone with a moving bed filter. Powder Technol. 399, 116941. https://doi.org/10.1016/j.powtec.2021.10.049.

Chang, M., Fan, Y., Lu, C., 2022b. Intrusive sampling of dust deposition in a granular bed filter-cyclone purifier. Chem. Eng. Sci. 260, 117824. https://doi.org/10.1016/j.ces.2022.117824.

Chang, M., Fan, Y., Lu, C., 2024. Filtration of dust particulates with a granular bed filter in novel coupled separator. Separ. Purif. Technol., 126502 https://doi.org/10.1016/j.seppur.2024.126502.

Chen, J.Y., 2007. On Separation Theory and Optimum Design of tangential–inlet reverse–flow Cyclone Separators.. Ph.D. Dissertation. China University of Petroleum (Beijing), pp. 99–107.

Colver, G.M., Brown, R.C., Shi, H., et al., 2002. Improving Efficiency of a Counter–current Flow Moving Bed Granular Filter. Office of Scientific & Technical Information Technical Reports, USA.

de la Campa, A.M., Moreno, T., de la Rosa, J., Alastuey, A., Querol, X., 2011. Size distribution and chemical composition of metalliferous stack emissions in the San Roque petroleum refinery complex. J. Hazard Mater. 190 (1–3), 713–722. https://doi.org/10.1016/j.jhazmat.2011.03.104.

Gambino, M., Vesely, M., Filez, M., Oord, R., Ferreira Sanchez, D., Grolimund, D., Nesterenko, N., Minoux, D., Maquet, M., Meirer, F., Weckhuysen, B.M., 2020. Nickel poisoning of a cracking catalyst unravelled by single-particle X-ray fluorescence-diffraction-absorption tomography. Ang. Chem.-Int. Ed. 59 (10), 3922–3927. https://doi.org/10.1002/ange.201914950.

Hoffmann, A.C., Stein, L.E., 2007. Gas cyclones and swirl tubes principles, design, and operation. Appl. Mech. Rev. 56 (2), B28. https://doi.org/10.1007/978-3-540-74696-6.

Klimpel, R.R., 1982. The influence of a chemical dispersant on the sizing performance of a 24-in. hydrocyclone. Powder Technol. 31, 255–262. https://doi.org/10.1016/0032-5910(82)89013-x.

Liu, F., Sun, G., Chen, J., 2012. Performance experiment and application of two–stage cyclone separators for oil shale particles. J. China Univer. Petrol. (Edition of Natural Science) 36 (6), 113–117. https://doi.org/10.3969/j.issn.1673–5005.2012.06.021 (in Chinese).

Lu, C., Gao, S., Fan, Y., et al., 2020. Separation Device. US 10758921.

Minkov, L., Dueck, J., Neesse, T., 2014. Computer simulations of the Fish-Hook effect in hydrocyclone separation. Miner. Eng. 62, 19–24. https://doi.org/10.1016/j.mineng.2013.10.003.

Mothes, H., Loffler, F., 1984. Motion and deposition of particles in a cyclone. Chem. Ing. Tech. 56, 714–715.

Noh, S., Heo, J., Woo, S., Kim, S., 2018. Performance improvement of a cyclone separator using multiple subsidiary cyclones. Powder Technol. 338, 145–152. https://doi.org/10.1016/j.powtec.2018.07.015.

Pendse, H., Tien, C., 2010. General correlation of the initial collection efficiency of granular filter beds. AIChE J. 28, 677–686. https://doi.org/10.1002/aic.690280421.

Roldán-Villasana, E.J., Williams, R.A., Dyakowski, T., 1993. The origin of the fish-hook effect in hydrocyclone separators. Powder Technol. 77, 243–250. https://doi.org/10.1016/0032-5910(93)85017-4.

Tong, J.S., 1985. Fluidized Drying Technology. China Architecture & Building Press, China.

Zhang, Y., Jiang, Y., Xin, R., Yu, G., Jin, R., Dong, K., Wang, B., 2023. Effect of particle hydrophilicity on the separation performance of a novel cyclone. Separ. Purif. Technol. 237, 116315. https://doi.org/10.1016/j.seppur.2019.116315.

Zhao, L., You, R., Liu, J., et al., 2024. A real-time measurement and analysis method for gas holdup in a wet scrubber with the use of image information entropy. Separ. Purif. Technol., 127255 https://doi.org/10.1016/j.seppur.2024.127255.